

## INFLUENCE OF SPUTTERING POWER ON PHYSICAL PROPERTIES OF NANOSTRUCTURED ZINC ALUMINUM OXIDE THIN FILMS FOR PHOTOVOLTAIC APPLICATIONS

B. RAJESH KUMAR<sup>a,b\*</sup>, T. SUBBA RAO<sup>b</sup>

<sup>a</sup>Department of Physics, Sri Venkateswara University, Tirupati-517502, A.P, India

<sup>b</sup>Materials Research Lab, Department of Physics, S.K. University, Anantapur-515003, India

In the present work Zinc Aluminum Oxide (ZAO) thin films have been deposited on glass substrates by DC reactive magnetron sputtering technique at different sputtering powers of Zn varied from 85 W - 125 W. XRD patterns exhibits ZAO thin films had a diffraction peak corresponding to (0 0 2) preferred orientation with c-axis perpendicular to the substrate surface. The preferred orientation is due to the lowest surface free energy for (0 0 2) plane. The minimum resistivity of  $1.67 \times 10^{-4} \Omega \cdot \text{cm}$  is found for the thin film deposited at sputtering power of 115 W. Optical absorption edge of nanostructured ZAO thin films has a significant blue shift to the region of higher photon energy. Such a shift is attributed to the Burstein-Moss effect. The optical band gap of nanostructured ZAO thin films is found to be in the range of 3.43 - 3.60 eV. The carrier concentration of ZAO thin films is found to be in the range of  $3.95 \times 10^{20} \text{ cm}^{-3}$  -  $1.38 \times 10^{21} \text{ cm}^{-3}$ .

(Received April 12, 2012; Accepted July 25, 2012)

*Keywords:* ZAO thin films; DC magnetron sputtering; Electrical resistivity; Optical transmittance

### 1. Introduction

Transparent conducting oxides (TCOs) have a range of highly useful applications as transparent electrodes in optoelectronic devices such as solar cells and flat panel displays. TCO coatings are essential for solar cell applications since they constitute a fundamental part in the emerging new generations of photovoltaic devices. The properties of TCO films includes large band gap ( $>3$  eV), low resistivity ( $10^{-3}$  -  $10^{-4} \Omega \cdot \text{cm}$ ) and a very good optical transmittance (80 - 90%) in the visible range. Though ITO film is extensively applied to photovoltaic devices and flat panel display because of its good electrical and optical properties, it has some problems such as high cost, low stability to  $\text{H}_2$  plasma and toxicity. Recently Al doped zinc oxide films has attracted much attention as a transparent and conductive film materials because it exhibits a wide band gap, high transparency and low resistivity. Zinc Aluminum Oxide (ZAO) has a lot of advantages such as non-toxicity, low cost and high stability against hydrogen plasma [1-6].

ZAO thin films have been prepared by several techniques such as RF sputtering process, evaporation, sol-gel method, pulsed laser deposition, chemical vapor deposition [7-10]. Among these processes, the sputtering process is one of the best methods for preparation of ZAO films because it has a lot of advantages such as low substrate temperature, good surface roughness, and low cost [11-14]. The objective of the present work is focused on the influence of sputtering power on structural, electrical and optical properties of ZAO thin films prepared by DC reactive magnetron sputtering. This paper reports the first observation of ZAO thin films sputtered by taking two individual metal targets of Zn and Al.

---

\*Corresponding author: rajphyind@gmail.com

## 2. Experimental details

Zinc Aluminum Oxide (ZAO) thin films were prepared by DC reactive magnetron sputtering technique. High purity of Zinc (99.999%) and Aluminum (99.99%) targets with 2 inch diameter and 4 mm thickness are used for deposition on glass substrates. The base pressure in chamber was  $3 \times 10^{-4}$  Pa and the distance between target and substrate was set at 60 mm. The glass substrates were ultrasonically cleaned in acetone and ethanol, rinsed in an ultrasonic bath in deionized water for 15 min, with subsequent drying in an oven before deposition. High purity (99.99%) Ar and O<sub>2</sub> gas was introduced into the chamber and was metered by mass flow controllers for a total flow rate fixed at 25 sccm. Deposition was carried out at a working pressure of 1 Pa after pre-sputtering with argon for 10 min. The depositions were carried out at different sputtering powers varied from 85 W to 125 W. Film thickness was measured by Talysurf thickness profilometer. The resulting thicknesses of the films were found to be ~300 nm respectively. X-ray diffraction (XRD) patterns of the films were recorded with the help of Philips (PW 1830) X-ray diffractometer using CuK $\alpha$  radiation. The tube was operated at 30 KV, 20mA with the scanning speed of 0.030(2 $\theta$ )/sec. The resistivities of the films ( $\rho$ ) were measured using the four-point probe method. Surface morphology of the samples has been studied using HITACHI S-3400 Field Emission Scanning Electron Microscope (FESEM) with Energy Dispersive Spectrum (EDS). EDS is carried out for the elemental analysis of prepared thin films. Optical transmittance of the films was recorded as a function of wavelength in the range of 300 – 1200 nm using JASCO Model V-670 UV-Vis-NIR spectrophotometer (Tokyo, Japan).

## 3. Results and discussion

### 3.1 Structural properties

Figure 1 shows the XRD patterns of ZAO films deposited on glass substrates. The XRD patterns reveal that all of the films are oriented with their c-axes perpendicular to the substrate plane having a hexagonal lattice structure. The diffraction peaks shifts from 34.31° to 34.74° towards higher angles compared with pure ZnO film. These shifts indicate the presence of a stress state in deposited films. This can be due to the incorporation of the Al as dopant in the ZnO lattice due to the different ionic radii of Al<sup>3+</sup> ( $r_{Al^{3+}} = 0.054$  nm) and Zn<sup>2+</sup> ( $r_{Zn^{2+}} = 0.074$  nm). The crystallite size was evaluated from the full-width-half-maximum (FWHM) value of the (0 0 2) reflections using the Scherrer equation [15]:

$$D = \frac{0.9\lambda}{\beta \cos\theta} \quad (1)$$

Where D is the crystallite size in nm,  $\lambda$  is X-ray wavelength (0.154 nm),  $\theta$  is the Bragg angle in degrees, and  $\beta$  is the FWHM of (0 0 2) plane. The crystallite size decreases with increase of sputtering powers of Zn. As sputtering power increased, the crystallite size decreased from 34.6 nm – 13 nm. The lattice constants and the film stress of ZAO thin films are obtained from XRD data. The lattice constant c can be evaluated by the following formula [16]:

$$\frac{1}{d_{hkl}^2} = \frac{4}{3} \left( \frac{h^2 + hk + k^2}{a^2} \right) + \frac{1}{c^2} \quad (2)$$

Where a and c are the lattice constants, and  $d_{hkl}$  is the crystalline plane distance for indices (h k l). It was found that all d values are larger than that of standard ZnO powder  $d_o$ , which is equal to 0.2603 nm. According to Eq. (2), the lattice constant c is equal to 2d for the (0 0 2) diffraction peak. Compared with the zinc oxide powders [17], all the ZAO thin films in our experiment exhibit discrepancy in d-value, which is due to the variation of residual stress developed in the films.

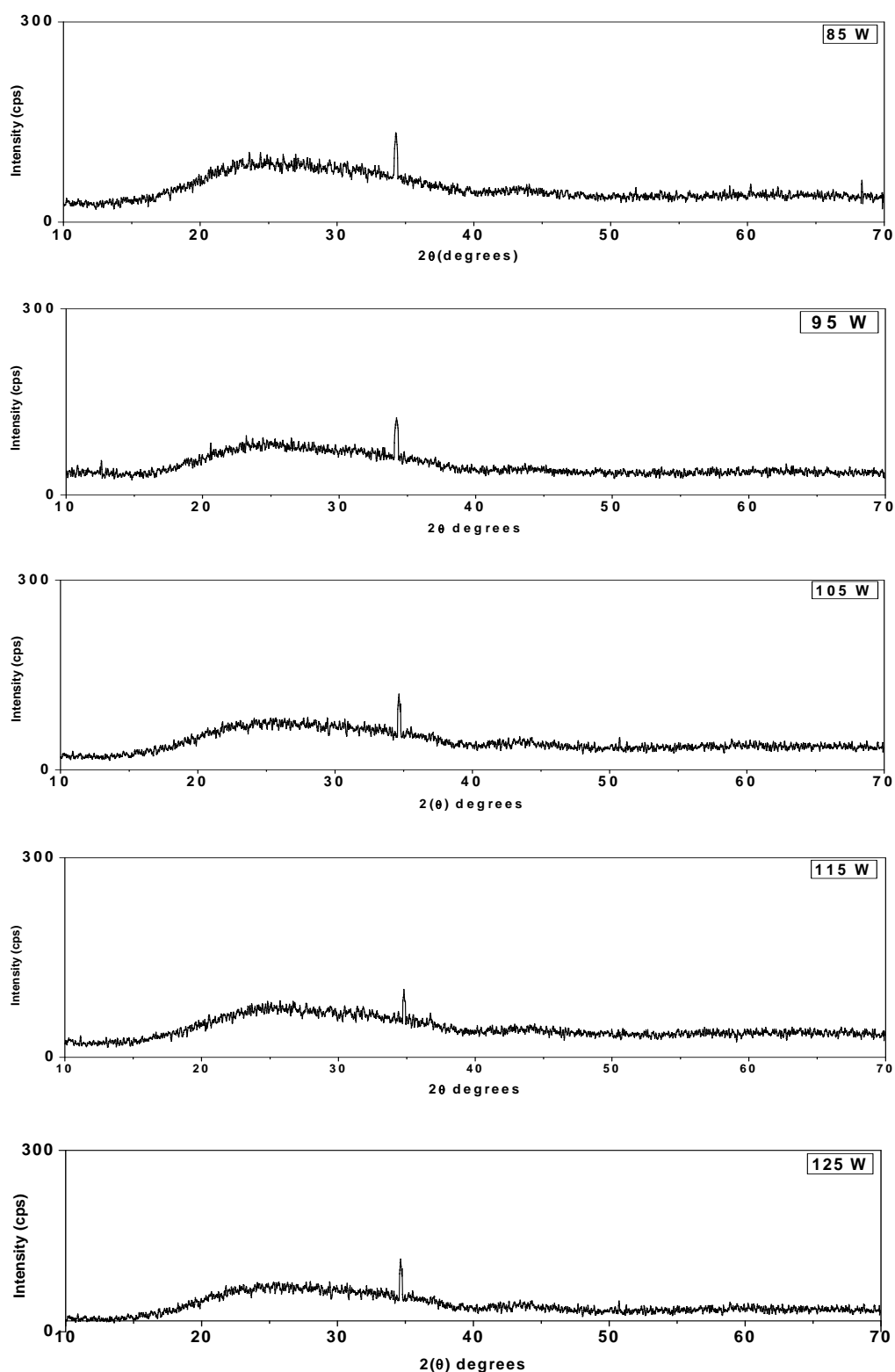


*Fig. 1 XRD patterns for ZAO thin films prepared with various sputtering powers of Zn.*

The stresses of the ZAO films were mainly induced by the energetic bombardment of the negative oxygen ions and the recoiling Ar atoms in high power sputtering condition. The film stress can be calculated based on the biaxial strain model [18]. The strain of the films in the

direction of c-axis as determined by XRD is  $\varepsilon = (c_{\text{film}} - c_0)/c_0$ , where  $c_0$  (0.5205 nm) is unstrained lattice parameter measured from ZnO powder.

The films stress  $\sigma_{\text{film}}$  parallel to the films surface can be derived by the following formula, which is valid for a hexagonal lattice [19]:

$$\sigma_{\text{film}} = \frac{2c_{13}^2 - c_{33}(c_{11} + c_{12})}{2c_{13}} \times \frac{c_{\text{film}} - c_0}{c_0} \quad (3)$$

For the elastic constants  $c_{ij}$ , data of single-crystalline ZnO have been used  $c_{11} = 208.8$ ,  $c_{33} = 213.8$ ,  $c_{12} = 119.7$ ,  $c_{13} = 104.2$  GPa. The following numerical relation for the stress derived from XRD can be obtained:

$$\sigma_{\text{film}} = -232.8 \times \varepsilon \text{ (GPa)} \quad (4)$$

The negative sign equation (4) corresponds to compressive stress. The film stress increases with increasing sputtering powers. The films sputtered at 85 W and 95 W are subjected to a compressive stress in c-axis direction, whereas the films sputtered at 105 W, 115 W and 125 W have tensile stress. The films deposited at higher sputtering power are stressed in comparison to those obtained at lower sputtering power. The possible reason for these variations may be due to the collision process during their growth. The structural parameters of ZAO thin films deposited on glass substrate at various sputtering powers are tabulated in Table 1.

*Table 1: Structural properties of nanostructured ZAO thin films deposited at different sputtering powers of Zn*

Sputtering power (Watts)	$2\theta$ (°)	FWHM (°)	Interplanar spacing $d_{002}$ (nm)	c-lattice constant (nm)	Crystallite size D (nm)	Stress $\sigma_{\text{film}}$ (GPa)
85	34.31	0.24	0.2611	0.5222	34.6	-0.98
95	34.40	0.32	0.2604	0.5208	26	-0.36
105	34.60	0.36	0.2590	0.5180	23.1	0.90
115	34.68	0.48	0.2583	0.5166	17.3	1.52
125	34.74	0.64	0.2592	0.5184	13	0.72

Fig. 2(a) - 2(e) shows Scanning electron microscopy (SEM) images of ZAO thin films deposited on glass substrate at different sputtering powers. As the sputtering power increases, the grains begin to grow loosely. It is clearly observed that the thin films have some rugged and irregular structures on the surface at higher sputtering power. The atomic percentages of Zn, Al and O determined by EDS are shown in the figure 3(a) - 3(e).

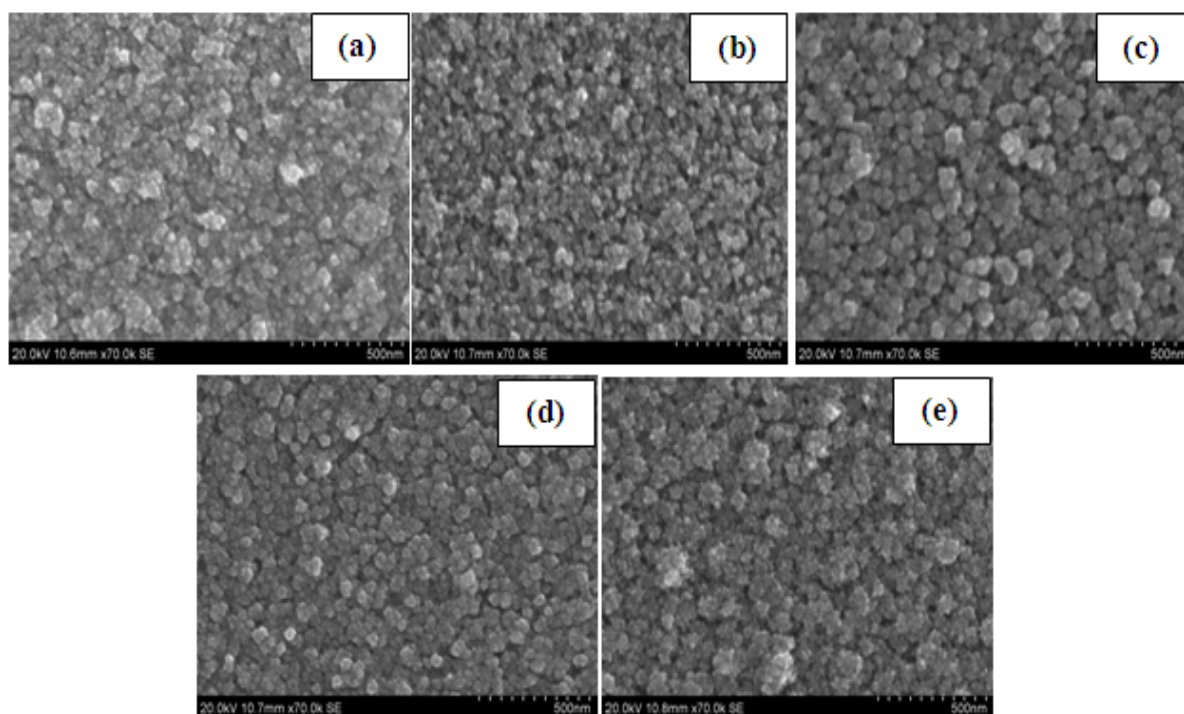


Fig. 2 Scanning Electron Microscopy (SEM) images of nanostructured ZAO thin films deposited on glass substrates with sputtering powers of (a) 85 W (b) 95 W (c) 105 W (d) 115 W and (e) 125 W.

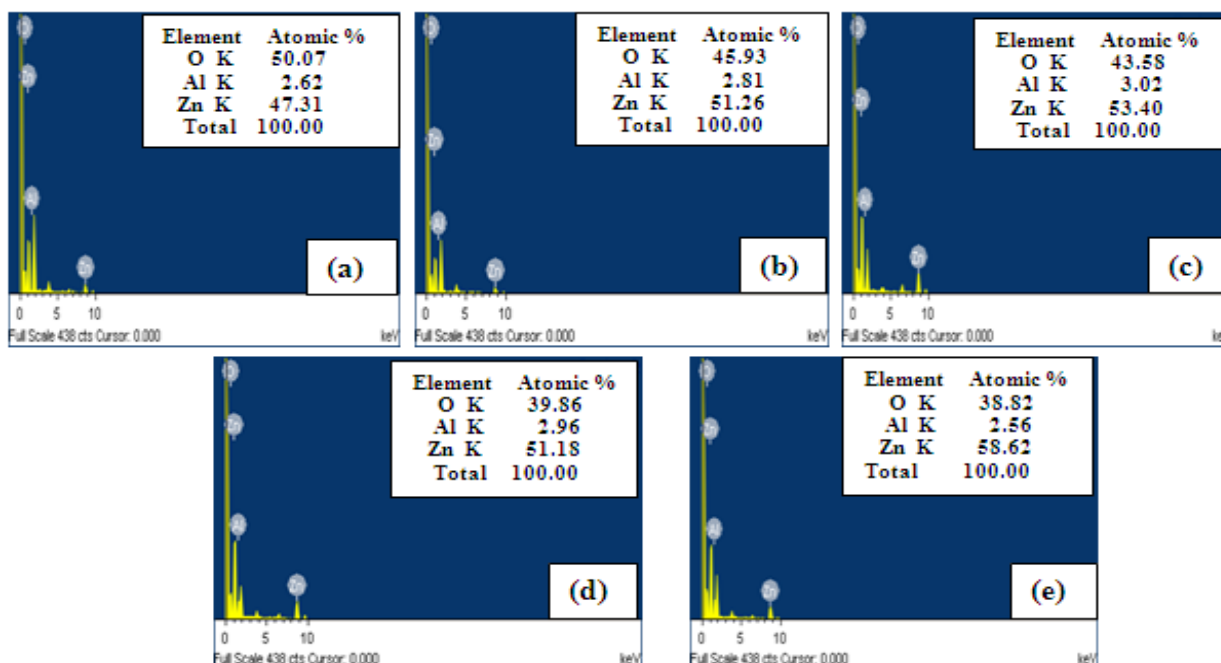


Fig. 3 EDS plots of ZAO thin films deposited on glass substrates with sputtering powers of (a) 85 W (b) 95 W (c) 105 W (d) 115 W and (e) 125 W.

The two-dimensional (2D) and three-dimensional (3D) views of the surface morphology of ZAO thin films are shown in figure 4(a) – 4(e), respectively. It is observed that the grains grow uniformly with homogenous distribution. The morphology of the films is continuous and dense.

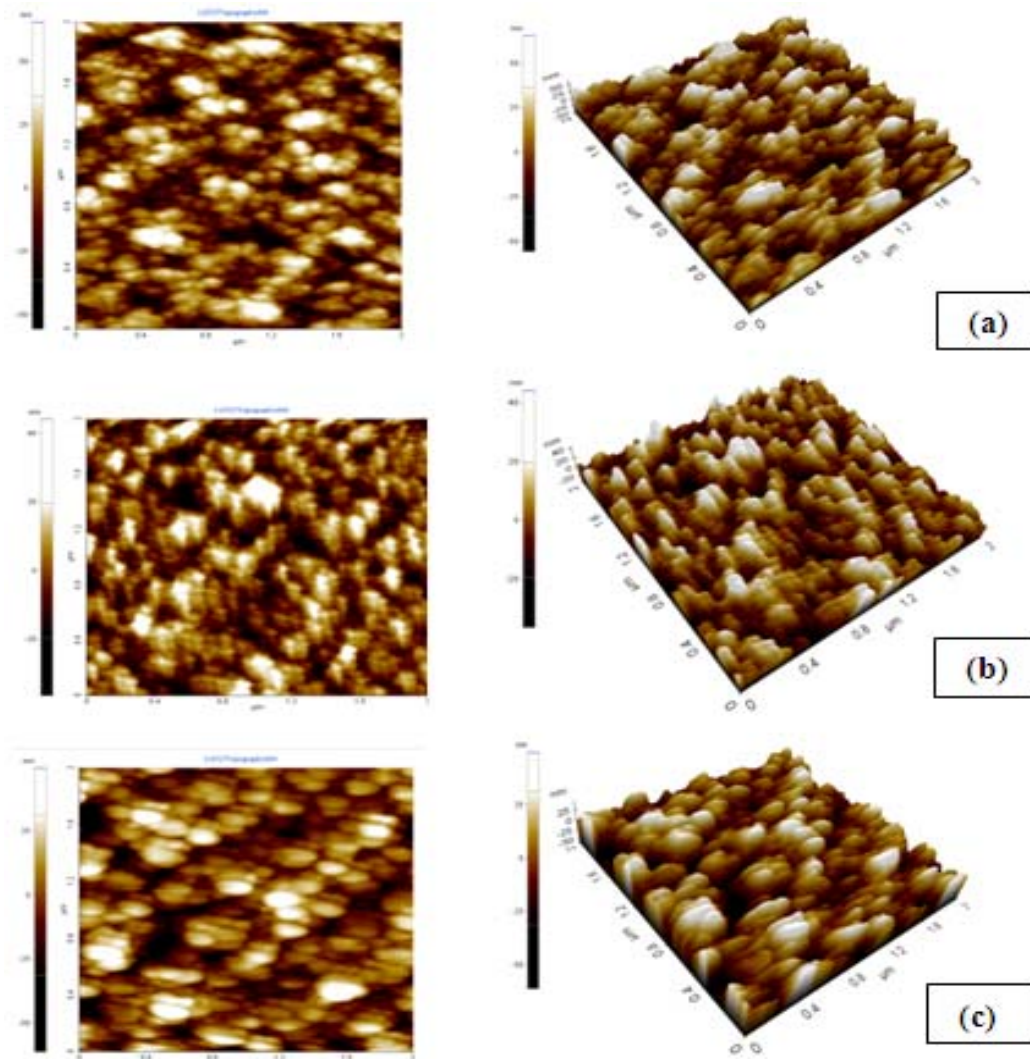
The root-mean-square (rms) surface roughness was measured over an area of  $2 \times 2 \mu\text{m}^2$  for all figures.

The RMS average roughness of a surface was calculated from an integral of the height profile following equation:

$$R_q = \sqrt{\frac{1}{N} \sum_{n=1}^N r_n^2} \quad (5)$$

Here,  $N$  is the number of data and  $r_n$  is the surface height in the  $n^{\text{th}}$  datum.

The root-mean-square (rms) surface roughness of the ZAO thin films sputtered at sputtering powers of 85 W, 95 W, 105 W, 115 W and 125 W are 7.02 nm, 8.07 nm, 11.07 nm, 13.42 nm and 18.54 nm respectively. As the sputtering power increases, the root-mean-square (rms) surface roughness of the thin films increases.



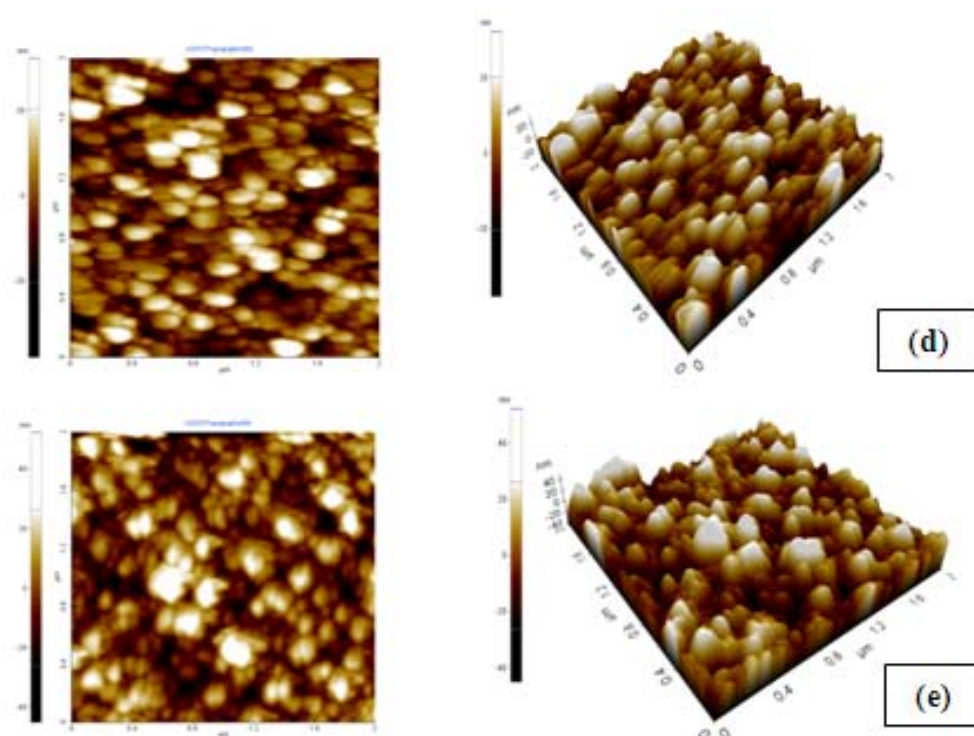


Fig. 4 AFM images of ZAO thin films deposited by sputtering with sputtering power of (a) 85 W (b) 95 W (c) 105 W (d) 115 W and (e) 125 W.

### 3.2 Electrical properties

The electrical resistivity of the ZAO films was investigated by four-point probe method at room temperature. Figure 5 shows the variation of the resistivity of ZAO films deposited at different sputtering powers. The experimental results show that the resistivity of ZAO film is significantly reduced when the DC power is increased from 85 W to 125 W. The decrease of resistivity is related to the increase of carrier concentration. The lowest resistivity of  $1.67 \times 10^{-4} \Omega \cdot \text{cm}$  is obtained for the thin film deposited at sputtering power of 115 W. The electrical conductivity in ZAO films is higher than that of pure ZnO film, due to the contribution from Al ions on substitutional sites of Zn ions and Al interstitial atoms, as well as from oxygen vacancies and Zn interstitial atoms.

The sheet resistance of the film ( $R_s$ ) was calculated using the equation

$$R_s = \frac{\rho}{t} \Omega/\text{sq} \quad (6)$$

where  $t$  is the film thickness. The sheet resistance values for 85 W, 95 W, 105 W, 115 W and 125 W are 15.1  $\Omega/\text{sq}$ , 9.5  $\Omega/\text{sq}$ , 6.0  $\Omega/\text{sq}$ , 4.7  $\Omega/\text{sq}$  and 4.8  $\Omega/\text{sq}$ . The sheet resistance decreases with increase of sputtering power. The lowering of the sheet resistance was caused by both the improvement of crystalline structure and the increase of free electron concentration supported by optical measurements.

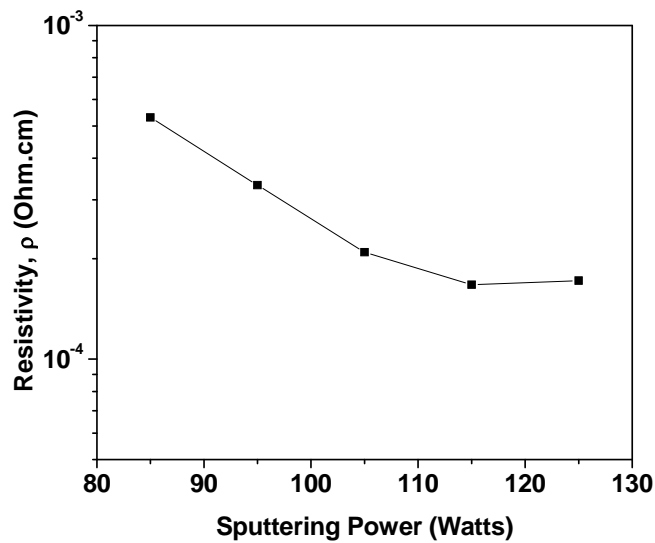


Fig. 5 Electrical resistivity of ZAO thin films as a function of sputtering powers.

### 3.3 Optical properties

Figure 6 shows the optical transmission spectra of ZAO thin films deposited at various sputtering powers. The average optical transmittance increases with increase of sputtering power, the maximum average optical transmittance is exhibited by the thin film deposited at 105 W with transmittance of 92%. But the thin film deposited at 115 W have a minimum resistivity of  $1.67 \times 10^{-4} \Omega \cdot \text{cm}$  with transmittance  $>90\%$  which can be used in photovoltaic devices as front electrode.

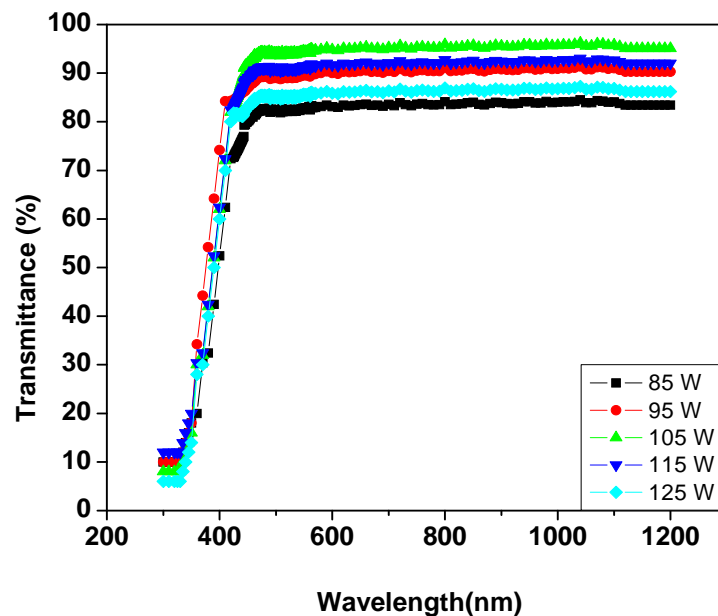


Fig. 6 Optical transmittance spectra of ZAO films deposited with various sputtering powers

The absorption coefficient  $\alpha$  is calculated using Lambert's law

$$\alpha = \frac{\ln\left(\frac{1}{T}\right)}{t} \quad (5)$$

where  $T$  is transmittance and  $t$  is the film thickness. The absorption is maximum at a high energy and decreases with optical energy in a manner similar to the absorption edge of semiconductors. Assuming that transition becomes constant at the absorption edge, the absorption coefficient  $\alpha$  for directly allowed transition for simple parabolic scheme can be ascribed as a function of incident photon energy. The optical band gap,  $E_g$  is determined from the dependence of absorption coefficient values ( $\alpha$ ) on the photon energy, using Tauc's relation [20]

$$(\alpha h\nu) = B(h\nu - E_g)^n \quad (6)$$

where  $B$  is a parameter that depends on the transition probability,  $E_g$  is the optical band gap energy of the material,  $h\nu$  is the photon energy and  $n$  is an index that characterizes the optical absorption process and is theoretically equal to 2 and  $\frac{1}{2}$  for indirect and direct allowed transitions respectively. The optical band gap of the films was evaluated from the Tauc's plot of  $(\alpha h\nu)^2$  versus  $h\nu$  shown in figure 7. The absorption edge of the transmittance shifted to the shorter wavelength (blue-shift) region. The optical band gap increases with increase of sputtering power from 3.43 eV to 3.60 eV shown in figure 8. The increase in optical band gap may be attributed to Burstein-Moss shift [21, 22] which occurs owing to filling up of low energy levels by the optical conduction electron. The studies of carrier concentration using UV-Vis-NIR spectrophotometer measurement data are reported in the literatures [23, 24].

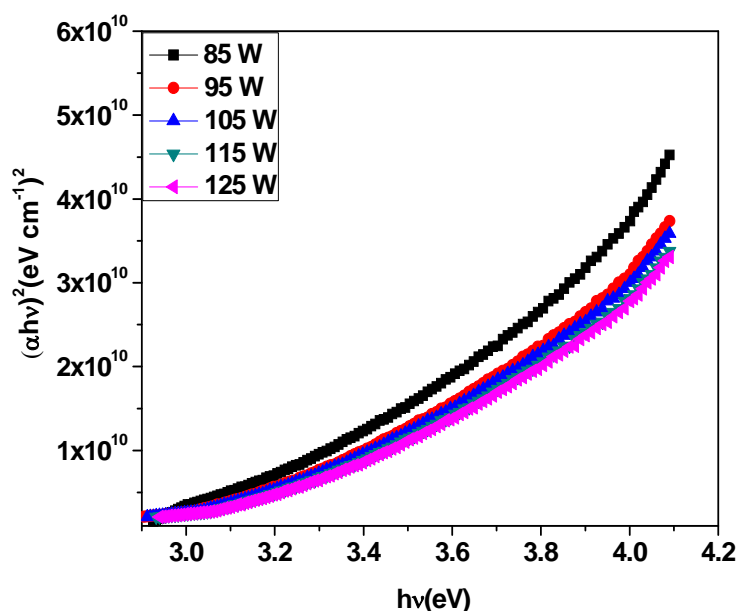


Fig. 7  $(\alpha h\nu)^2$  versus  $h\nu$  plots for ZAO thin films deposited at various sputtering powers of Zn.

The Burstein-Moss effect explained the broadening of band gap energy with the increasing of carrier concentration. The electron concentration could be calculated by the shift of band gap energy as shown in equation

$$\Delta E^{BM} = \left( \frac{h^2}{8m^*} \right) \left( \frac{3N}{\pi} \right)^{\frac{3}{2}} \quad (7)$$

where  $\Delta E^{BM}$  is the energy band gap broadening,  $h$  is the Planck constant,  $m^*$  is the effective mass of the electron and  $N$  is the carrier concentration. The carrier concentration is found to be in the range of  $3.29 \times 10^{20} \text{ cm}^{-3} - 1.38 \times 10^{21} \text{ cm}^{-3}$

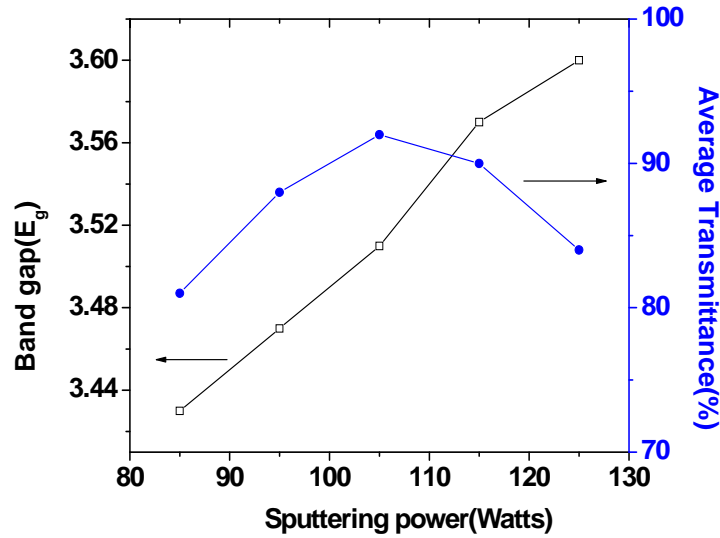


Fig. 8 Optical band gap and average visible transmittance of ZAO thin films as a function of sputtering powers.

Figure of merit ( $\Phi$ ) is the quantity to judge the quality of the transparent conducting oxide films. The figure of merit of the films was evaluated from the optical transmittance and sheet resistance ( $R_s$ ) using the Haacke's relation [25].

$$\Phi (\Omega^{-1}) = \frac{T^{10}}{R_s} \quad (8)$$

where  $T^{10}$  is the average optical transmittance and  $R_s$  is the sheet resistance.

The best figure of merit with  $7.3 \times 10^{-2} \Omega^{-1}$  and sheet resistance of  $4.7 \Omega/\text{sq}$  is obtained for the film sputtered at 115 W.

#### 4. Conclusions

Zinc Aluminum Oxide thin films have been deposited on glass substrates by DC reactive magnetron sputtering technique at different sputtering powers varied from 85 W to 125 W. The influence of sputtering power on the structural, electrical and optical properties of sputtered ZAO films was investigated. The sputtering power in our deposition system strongly affected the properties of ZAO film. All the ZAO films have (0 0 2) preferred orientation with the c-axis perpendicular to the substrate. The minimum resistivity of  $1.67 \times 10^{-4} \Omega \cdot \text{cm}$  and optical transmittance of 90% is obtained for the thin films deposited at 115 W. The blue shift of the absorption edge with the increasing sputtering power is mainly attributed to the Burstein-Moss effect, since the absorption edge of a degenerate semiconductor is shifted to shorter wavelengths with increasing carrier concentration. For a conclusion we achieved ZAO thin film with excellent

crystallinity, low resistivity and high transmittance which can be used in photovoltaic devices as front electrode.

### Acknowledgements

The authors are thankful to UGC, New Delhi, India for financial support under the major research project (F.NO.37-346/2009, SR).

### References

- [1] X.J. Jiang, F.L.Wong, M.K.Fung, S.T.Lee, *Appl.Phys. Lett.* **83**, 1875 (2003).
- [2] Z.L.Pei, C.Sun, M.H.Tan, J.Q.Xiao, D.H.Guan, R.F.Huang, L.S.Wen, *J.Appl.Phys.* **90**, 3432 (2001).
- [3] R.Cebulla, R.Wendt, K.Ellmer, *J.Appl.Phys.* **83**, 1087 (1998).
- [4] E.G.Fu, D.M.Zhuang, G.Zhang, M.Zhao, W.F.Yang, J.F. Liu, *Microelectron. J.* **35**, 383 (2004).
- [5] D.Song, A.G.Aberle, J.Xia, *Appl.Surf.Sci.* **195**, 291 (2002).
- [6] J.M.Ting, B.S.Tsai, *Mater.Chem. Phys.* **72**, 273 (2001).
- [7] F.Quaranta, A.Valentini, F.R.Rizzi, *J.Appl.Phys.* **74**, 247 (1993).
- [8] M.Ohyama, H.Kozuka, T.Yoko, *Thin Solid Films* **306**, 78 (1997).
- [9] V.Cracium, J.Elders, J.G.E.Gardeniers, *Appl.Phys.Lett.* **65**, 2963 (1994).
- [10] S.K.Ghandhi, R.J.Field, J.R.Shealy, *Appl.Phys.Lett.* **37**, 449 (1980).
- [11] S.S.Lin, J.L.Huang, D.F.Lii, *Surf.Coat.Technol.* **176**, 173 (2004).
- [12] F.K.Shan, Y.S.Yu, *J.Eur.Ceram.Soc.* **24**, 1869 (2004).
- [13] D.H.Zhang, Q.P.Wang, Z.Y.Xue, *Appl.Surf.Sci.* **207**, 20 (2003).
- [14] Q.P.Wang, D.H.Zhang, H.L.Ma, Z.H.Zhang, X.J.Zhang, *Appl.Surf.Sci.* **220**, 12 (2003).
- [15] B.D.Cullity, *Elements of X-ray diffraction*, Addition-Wesley, London, 99 (1959).
- [16] G.J.Fang, D.J.Li, B.L.Yao, *Phys.Stat.Sol.A* **193**, 139 (2002).
- [17] H.Kim, A.Pique, J.S.Horwitz, H.Murata, *Thin Solid Films* **377**, 798 (2000).
- [18] A.Segmuller, M.Murakami, R.Roscoberg, *Analytical Techniques for Thin Films*, Academic Press, Boston, 143 (1988).
- [19] R.Cebulla, R.Wendt, K.Ellmer, *J.Appl.Phys.* **83**, 1087 (1998).
- [20] J. Tauc, R. Grigorovici, A. Vancu, *Phys.Stat.Sol.* **15**, 627 (1966).
- [21] E.Burstein, *Phys.Rev.* **93**, 632 (1954).
- [22] T.S.Moss, *Optical properties of semiconductors*, Butterworth and Co Pub. Ltd, London (1961).
- [23] S.Bandyopahdyay, G.K.Paul and S.K.Sen, *Sol. Energy Mater. Sol. Cells*, **71**, 106 (2002).
- [24] T.A.Vijayan, R.Chandramohan, S.Valanarsu, J.Thirumalai and S.P.Subramanian, *J.Mater. Sci.* **43**, 1780 (2008).
- [25] G. Haacke, *J. Appl. Phys.* **47**, 4086 (1976).